Bulletin of the Seismological Society of America, Vol. 96, No. 2, pp. 427–445, April 2006, doi: 10.1785/0120050015

The Estimation of Minimum-Misfit Stochastic Models from Empirical Ground-Motion Prediction Equations

by Frank Scherbaum, Fabrice Cotton, and Helmut Staedtke

Abstract In areas of moderate to low seismic activity there is commonly a lack of recorded strong ground motion. As a consequence, the prediction of ground motion expected for hypothetical future earthquakes is often performed by employing empirical models from other regions. In this context, Campbell's hybrid empirical approach (Campbell, 2003, 2004) provides a methodological framework to adapt ground-motion prediction equations to arbitrary target regions by using response spectral host-to-target-region-conversion filters. For this purpose, the empirical ground-motion prediction equation has to be quantified in terms of a stochastic model. The problem we address here is how to do this in a systematic way and how to assess the corresponding uncertainties. For the determination of the model parameters we use a genetic algorithm search. The stochastic model spectra were calculated by using a speed-optimized version of SMSIM (Boore, 2000). For most of the empirical ground-motion models, we obtain sets of stochastic models that match the empirical models within the full magnitude and distance ranges of their generating data sets fairly well. The overall quality of fit and the resulting model parameter sets strongly depend on the particular choice of the distance metric used for the stochastic model. We suggest the use of the hypocentral distance metric for the stochastic simulation of strong ground motion because it provides the lowest-misfit stochastic models for most empirical equations. This is in agreement with the results of two recent studies of hypocenter locations in finite-source models which indicate that hypocenters are often located close to regions of large slip (Mai *et al.*, 2005; Manighetti *et al.*, 2005). Because essentially all empirical ground-motion prediction equations contain data from different geographical regions, the model parameters corresponding to the lowest-misfit stochastic models cannot necessarily be expected to represent single, physically realizable host regions but to model the generating data sets in an average way. In addition, the differences between the lowest-misfit stochastic models and the empirical ground-motion prediction equation are strongly distance, magnitude, and frequency dependent, which, according to the laws of uncertainty propagation, will increase the variance of the corresponding hybrid empirical model predictions (Scherbaum *et al.*, 2005). As a consequence, the selection of empirical ground-motion models for host-to-target-region conversions requires considerable judgment of the ground-motion analyst.

Introduction

The site-dependent assessment of expected ground motions and their variabilities for hypothetical future earthquakes is a key element of any seismic hazard analysis. In areas of moderate to low seismic activity, such as in the central and eastern United States or in many regions of Europe, indigenous strong ground motion models rarely exist. As a consequence, strong ground motion prediction has to be performed by either calculating synthetic seismograms based on physical models or by employing empirical models from other areas. Because of the large number of existing empirical ground-motion equations from high-seismicity regions (Douglas, 2003), the latter approach has become increasingly popular, in particular, in conjunction with a logic tree approach (Kulkarni *et al.*, 1984; Bommer *et al.*, 2005). However, the selection of appropriate models for a given study area is not straightforward and is often subject to personal preferences of the hazard analyst rather than to physical criteria. Some recent studies have started to address this problem and, as attempts toward transparent and consistent selection strategies, discuss the relevance and sensitivity of particular criteria to consistently compare and judge ground-motion models and to define branch weights based on measurable quantities rather than on vaguely defineable personal choices (Cotton *et al.*, 2006; Scherbaum *et al.*, 2004a; Bommer *et al.*, 2005). In this context, rather than trying to find ideally matching empirical relations, which in practice will always lead to imperfect results, Campbell (2003, 2004) proposes a methodological framework to transfer ground-motion models from their data host region to any arbitrary target region. A key element in this so-called hybrid empirical approach is the calculation of response-spectral transfer functions based on stochastic ground-motion models (Boore, 2003) for both the host and the target region. The purpose of this transfer function is the removal of the effects of the host region characteristics in terms of attenuation, geometrical spreading, average stress drop, etc., and their replacement by the equivalent effects for the target region. This can improve the overall usefulness of a particular empirical model for a target region of interest. Although Campbell (2003) quantitatively addresses both epistemic and aleatory uncertainty, both theoretically and practically in the development of a CEUS ground-motion relation, and although stochastic models have been developed for several regions (Boore, 1983; Boore and Atkinson, 1987; Ou and Herrmann, 1990; Boore *et al.*, 1992; Margaris and Boore, 1998; Malagnini *et al.*, 1999; Raoof *et al.*, 1999; Atkinson and Silva, 2000; Malagnini *et al.*, 2000; Bay *et al.*, 2003), model parameter uncertainties in these models are almost never quantified. As a consequence, the increased variability in the corresponding resulting ground-motion estimates after host-to-target-region conversion (due to the laws of uncertainty propagation) cannot be assessed either. Therefore, in the present study, we attempt to quantify optimum stochastic models and model parameter uncertainties for the host regions of a number of conventionally used empirical ground-motion prediction equations for shallow crustal earthquakes. This is seen as a first step toward achieving complete quantitative error tracking in host-to-target-region conversions. The corresponding problem for target-region characterizations using microearthquake records is discussed in Rietbrock *et al.* (unpublished manuscript, 2005). In a related article (Scherbaum *et al.*, 2005), we demonstrate that the contribution of model parameter uncertainties in host-to-target-region conversions to the overall variability in the resulting ground motion in composite models is considerable and can become a major portion of the overall epistemic uncertainty of ground-motion estimates. Note that the present article is not trying to evaluate or validate the hybrid empirical model of Campbell (2003). We simply treat this method here as a published, viable tool for which we attempt to determine model parameters for generating data sets of existing empirical ground-motion models in a systematic way. In addition to their use in the context of the hybrid empirical method, the models derived in this study might also be of use in the context of quantifying the upper bounds on earthquake ground motion for seismic hazard analysis (for a discussion of this issue, see Bommer *et al.*, 2004). Extrapolating stochastic models into the limits of physically still plausible ranges of model parameters may be considered a viable alternative to the practice of truncating ground motion in terms of standard deviation of the model, which is theoretically unjustified. Futhermore, the parameter sets might also be useful for the simulation of time histories consistent with the ground-motion models used in seismic hazard studies. Such time histories are needed, for example, to analyze nonlinear dynamic behavior of structures.

Method

The hybrid empirical method proposed by Campbell (2003) assumes that both the host region of the data set from which an empirical ground-motion prediction relation is derived as well as the target region in which the modified empirical models are going to be applied can be modeled by single point-source stochastic models (Boore, 1983, 2003). In the present study we determine sets of stochastic model parameters for the host regions of several popular ground-motion prediction relations (Ambraseys *et al.*, 1996; Sabetta and Pugliese, 1996; Abrahamson and Silva, 1997; Boore *et al.*, 1997; Spudich *et al.*, 1999; Berge-Thierry *et al.*, 2003; Lussou *et al.*, 2001; Ambraseys and Douglas, 2003; Campbell and Bozorgnia, 2003a, 2003b, 2003c, 2004). This particular set of models was selected to capture a wide range of shallow crustal host-region environments (Cotton *et al.*, 2006), initially for application of the hybrid empirical method to central Europe within the PEGASOS project (Abrahamson *et al.*, 2002). However, because the target-region models have to be specified separately, the models obtained here are believed to be useful for the application of the hybrid method to arbitrary target regions.

Because empirical ground-motion models are only rarely derived based on data sets from single geographical regions, the host region of an empirical ground-motion model has to be considered an apparent one, defined by regions of similar generalized tectonics. It will contain characteristics of different geographical regions. Therefore, we approach the determination of apparent host-region models as an inversion problem in which we use synthetic response spectra generated from each empirical ground-motion relation for various magnitudes and distances as "data" for which we determine optimum models. For the model parameter optimization we used a genetic algorithm search strategy (Goldberg, 1989).

Stochastic Host Region Model

The simulation of strong ground motion using the stochastic method goes back more than two decades. Based on the work of Hanks and McGuire (Hanks, 1979; McGuire and Hanks, 1980; Hanks and McGuire, 1981), Boore (1983), in his ground-breaking article proposed a simple, but powerful technique to simulate high-frequency ground-motion time series and response spectra for use in engineering seismology. Over the years, the method has seen numerous applications and public domain versions of Boore's SMSIM code (Boore, 2000) have been widely used. Although the method has been extended and modified in many details, the basic framework has remained essentially unchanged (Boore, 2003). According to Boore (2003), the total Fourier spectrum of ground motion as a function of seismic moment M_0, distance R, and frequency f can be described as:

$$Y(M_0, R, f) = E(M_0, f) \cdot P(R, f) \cdot G(f) \cdot I(f), \quad (1)$$

where $E(M_0, f)$ is the source, $P(R, f)$ is the path, and $G(f)$ is the site contribution, respectively. The instrument or type of motion is described by $I(f)$. Following Campbell (2003), for the purpose of host-region characterization we restrict ourselves to a single-corner frequency, ω-square source spectrum for which the corner frequency is given by

$$f_0 = 4.9 \cdot 10^6\ \beta_S(\Delta\sigma/M_0)^{1/3} \quad (2)$$

(Brune, 1970, 1971). In equation (2), the corner frequency f_0 is given in hertz, the shear-wave velocity β_S in the source region is given in kilometers per second, stress parameter $\Delta\sigma$ is in bars, and seismic moment M_0 in dyne cm. The complete source spectrum $E(M_0, f)$ for this source type can be written as

$$E(M_0, f) = \frac{\langle R_{\Theta\Phi}\rangle \cdot V \cdot F}{4\pi \cdot \rho_S \cdot R_0 \cdot \beta_S^3} \cdot \frac{M_0}{1 + \left(\frac{f}{f_0}\right)^2}. \quad (3)$$

Here, $\langle R_{\Theta\Phi}\rangle$ is the average radiation pattern, V represents the energy partitioning into the two horizontal components ($1/\sqrt{2}$), F is the effect of the free surface (2 for *SH* waves), ρ_S and β_S are density and shear-wave velocity in the source regions, and R_0 is the reference distance for geometrical spreading (usually set to 1). The path effect $P(R, f)$ is modeled as the product of a damping function $A(R, f)$ and a geometrical spreading function $Z(R)$ as

$$P(r, f) = A(R, f) \cdot Z(R), \quad (4)$$

where

$$A(R, f) = e^{-\frac{\pi f R}{Q(f) \cdot c_Q}} \quad (5)$$

with shear-wave phase velocity c_Q. $Q(f)$ is the frequency-dependent quality factor modeled as $Q(f) = Q_0 \cdot f^{\alpha}$. In the present study, the geometrical spreading function $Z(R)$ is modeled as:

$$Z(R) = \begin{cases} \left(\frac{R_0}{R}\right)^{a_1} & \text{for } R \le R_1 \\ Z(R_1)\left(\frac{R_1}{R}\right)^{a_2} & \text{for } R_1 < R \le R_2 \\ Z(R_2)\left(\frac{R_2}{R}\right)^{a_3} & \text{for } R_2 < R \end{cases}. \quad (6)$$

The site spectrum $G(f)$ is modeled as

$$G(f) = T(vs_{30}, f) \cdot e^{-\pi\kappa_0 f}, \quad (7)$$

where $T(vs_{30}, f)$ is a generic rock site frequency-response function with vs_{30} (the shallow shear-wave velocity down to depths of 30 m) as controlling parameter. The corresponding velocity depth models are constructed such that for $vs_{30} =$ 620 and 2800 m/sec they converge to the western and eastern U.S. generic rock profiles of Boore and Joyner (1997), respectively. Their derivation is discussed in detail in Cotton *et al.* (2006). The empirical models were used for site conditions as close as possible to National Earthquake Hazards Reduction Program (NEHRP) site class B. The second term in equation (7) ($e^{-\pi\kappa_0 f}$) describes the distance-independent kappa-filter discussed by Anderson and Hough (1984). Since we are interested in response spectral amplitudes, the instrument frequency-response function $I(f)$ is modeled as a SDOF-oscillator response (compare, equation 22 in Boore [2003]). Based on the Fourier spectral representation given by equation (1), response spectral values are calculated by using random vibration theory (Boore and Joyner, 1984). In this context, the path duration is modeled as

$$T_p = r \cdot R, \quad (8)$$

where r is a free model parameter.

Model Parameter Optimization

Finding an acceptable set of model parameters for a particular stochastic host-region model can be thought of as an optimization problem in which a particular misfit function is minimized. For each empirical ground-motion prediction equation we first generate a set of synthetic response spectra that sample the complete magnitude, distance, and frequency range for which the authors claim the equation is valid. The goal of the inversion is to identify all models that give an acceptable misfit between predicted and observed data. However, geophysical inverse problems may have numerous distinct, acceptable solutions. The corresponding optimization problems may be characterized by a complicated surface for the misfit function in the solution parameter space. For exploring such a surface, direct inversion and simple random search methods are often inadequate. However, directed search methods such as the genetic algorithm (GA) (Goldberg, 1989) can be configured to balance convergent and random processes to find large sets of solutions that span the acceptable regions of complicated misfit surfaces.

The GA is a guided search technique that requires neither a linearized forward method nor a single starting model and which can be applied to very large model spaces. Consequently, fewer assumptions and physical approximations are required and a greater range of possible solutions is examined than with many other inversion methods. This technique has been used by many authors in geophysics (e.g., Stoffa and Sen, 1991; Hernandez *et al.*, 1999; Gentile *et al.*, 2004).

The GA method operates with successive generations of trial models. Beginning with a random initial population of models, succeeding generations are created by three stochastic processes: (1) selection (saving models with smaller misfits), (2) crossover (combining part of two models to form new trial models), and (3) mutation (making changes to models).

The GA used in this study was originally developed by Lomax and Snieder (1994, 1995). The code was interfaced with a speed-optimized version of the SMSIM code (Boore, 2000). The misfit is calculated as the L2-norm for the logarithmic spectra generated for the particular stochastic host-region model. We employ the GA to produce a large set of acceptable solutions and associated misfit values, in contrast to inversion for a single, "optimum" solution. The probabilities of crossover and mutation (compare, Goldberg, 1989) were chosen as 0.6 and 0.04, respectively. This tended to produce a diverse set of acceptable models, the scatter of which gives an estimate of uncertainty, resolution, and parameter trade-offs in the nonlinear inversion.

Because the inversion problem would not be well constrained if we used the complete set of stochastic model parameters as free parameters, during the optimization we used fixed values for the density and the shear-wave velocity (See Table 6). Following Campbell (2003), for the source model, a ω-square source model was used in all cases with the source duration fixed to $1/f_0$. The average radiation pattern was taken as 0.55.

To validate the inversion strategy, we tried to recover the model parameters of the WNA-model given by Campbell (2003) from synthetic response spectra calculated for the magnitude, distance, and frequency range for which the model of Abrahamson and Silva (1997) is valid. As can be seen in Table 1, the model parameters for the optimum model (model with the lowest misfit value) come very close to the model parameters that we used to generate the synthetic spectra. This demonstrates that with the chosen sampling of the magnitude, distance, and frequency space we obtain sufficient constraints on the parameters which we want to recover. To demonstrate how well the good models predict the input data in the whole frequency band, WNA-model spectra for selected magnitudes and distances, superimposed by the 25 best-fitting stochastic models obtained in the inversion are displayed in Figure 1.

Table 1
Model Parameter Search Range, True Model Values, and Minimum Misfit Values Obtained from the Inversion of Synthetic Response Spectra Calculated for the Parameters of the WNA Model of Campbell (2003)

Parameter	Search Range	True Model Value	Minimum Misfit Value
$\Delta\sigma$ (bar)	0.1 to 500	100	91.1
κ_0 (sec)	0 to 0.1	0.04	0.037
Q_0	50 to 1000	180	168.1
α	0 to 1.0	0.45	0.5
R_1 (km)	10 to 50	40	41.5
a_1	-0.8 to -1.2	-1	-0.98
r	0.02 to 0.08	0.05	0.058
vs_{30} (m/sec)	450 to 1000	620	620

All parameters not shown here were fixed at the values given in Campbell (2003).

Distance Metrics for Stochastic Simulation

Ground-motion prediction equations in engineering seismology attempt to provide ground-motion models for earthquakes in magnitude ranges for which the extension of the sources cannot be ignored. For extended sources, the part of the rupture plane being the source of the dominant strong ground motion is usually not known. Therefore, reduction of ground motion (both geometrical and anelastic) as a function of distance from the extended source becomes complicated, especially at short distances. As a consequence, different distance metrics have been suggested for use within the context of empirical ground-motion prediction equations (Reiter, 1990; Kramer, 1996; Abrahamson and Shedlock, 1997). Types and ranges of validity of the distance measures employed in the ground-motion models used in the present study are given in Table 2. Combining two or more ground-motion models within a seismic hazard study, for example, within a logic tree framework (Kulkarni *et al.*, 1984), will require a correction for differences in distance metrics (Bommer *et al.*, 2005). For this purpose, explicit distance conversion relations have been developed based on regression analysis on simulated data (Scherbaum *et al.*, 2004b). Regarding the distance measures employed for stochastic modelling of ground motion, an even larger diversity exists than for empirical ground-motion prediction equations. Among those metrics in use are the hypocentral distance R_{hyp} (Boore, 1986; Chen and Atkinson, 2002), the distance to the closest point on the rupture plane R_{rup} (Boore, 2003; Campbell, 2003), or R_{rup} combined with a pseudodepth chosen to be either magnitude dependent (Atkinson and Silva, 2000) or frequency dependent (Atkinson and Silva, 1997). Furthermore, Joyner-Boore distance combined with several types of pseudodepths have been used as well (Boore *et al.*, 1992, 1997; Margaris and Boore, 1998). In the test case discussed previously, this is not an issue because the forward and the inverse problem was solved with the same approach. For the determination of stochastic host-region models in

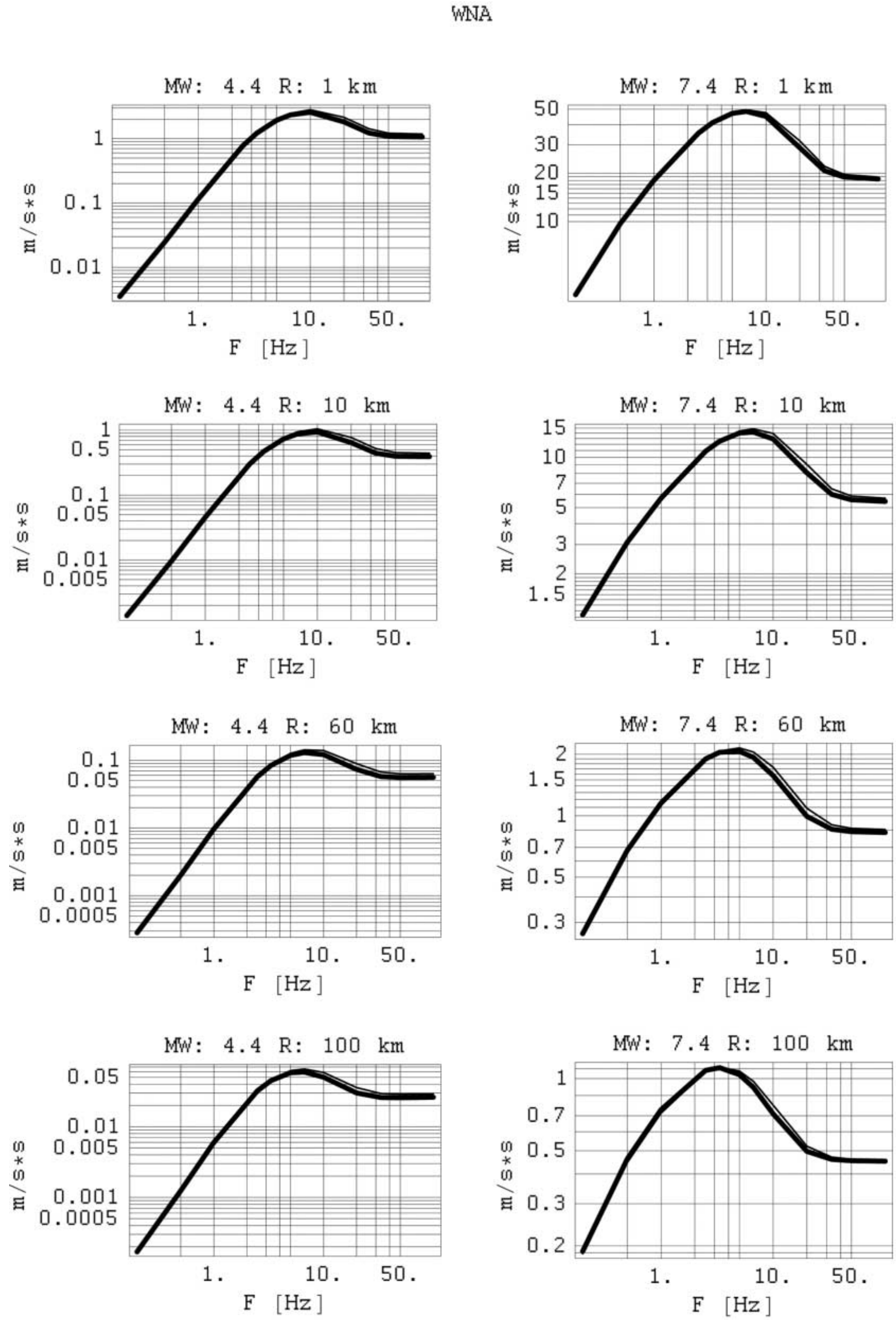

Figure 1. Acceleration-response spectra for the WNA model of Campbell (2003) for selected magnitudes and distances (heavy black lines) superimposed by the model spectra for the optimum stochastic obtained in the inversion (thin gray lines).

Table 2
Types and Ranges of Validity of Distance Metric, Magnitude, and Frequency for the Ground-Motion Models Used in This Study

Model Name	Distance Type*	Distance Range (km)	Magnitude Type	Magnitude Range	Frequency Range (Hz)
Abrahamson and Silva (1997)	R_{rup}	3–150	M_W	4.4–7.4	0.2–100
Ambraseys and Douglas (2003)	R_{JB}	≤ 15	M_S	4.8–7.8	0.5–10
Ambraseys *et al.* (1996)	R_{epi} ($M_S \leq 6$)/ R_{JB} ($M_S > 6$)	≤ 200	M_S	4.0–7.9	0.5–10
Berge-Thierry *et al.* (2003)	R_{hyp}	5–100	$M_S \leq 6$/ $M_W > 6$	4.0–7.3	0.1–34
Boore *et al.* (1997)	R_{JB}	≤ 80	M_W	5.5–7.5	0.5–10
Campbell and Bozorgnia (2003a)	R_{seis}	3–100	M_W	4.7–7.7	0.25–20
Lussou *et al.* (2001)	R_{hyp}	10–200	*M*-JMA	3.5–6.3	0.1–50
Sabetta and Pugliese (1996)	R_{JB} and R_{epi}	≤ 100	$M_L \leq 5.5$/ $M_S > 5.5$	4.6–6.8	0.25–25
Spudich *et al.* (1999)	R_{JB}	≤ 100	M_W	5.0–7.0	0.5–10

For the definitions of the distance types see Table 3.
*R_{epi} is the epicentral distance.

arbitrary cases, however, what distance metric to use is a nontrivial issue. For the present study, the distance conversion issue was addressed in the following way. First, we determined the distance range covered by each ground-motion prediction equation in terms of each instrinsic distance metric (e.g., rupture distance for Abrahamson and Silva, 1997). These validity ranges were subsequently expressed in terms of Joyner-Boore distances which we used as reference distance metric. The corresponding conversions were performed using the relations of Scherbaum *et al.* (2004b). The distance values for which synthetic spectra were subsequently calculated were defined in terms of the reference distance metric. Subsequently, for each of these reference distance values, all other distance metrics of interest were calculated, again using the conversion relations of Scherbaum *et al.* (2004b).

One could possibly expect that the distance metric that was used for the generation of an empirical prediction equation—in other words, for the regression analysis—would also provide the best-fitting stochastic models. This, however, turned out not to be the case. The heavy solid lines in Figure 2, for example, show spectra for selected magnitudes and Joyner-Boore distances calculated from the ground-motion prediction equation of Abrahamson and Silva (1997). Because the ground-motion prediction equation of Abrahamson and Silva (1997) is based on rupture distance, prior to the calculation of the model spectra, each of the selected reference distance values was converted into rupture distance using the conversion relations of Scherbaum *et al.* (2004b). The thin lines in Figure 2 show the corresponding model spectra for the minimum misfit stochastic model obtained by using rupture distances also for the stochastic model. For the lower bound of the magnitude validity range (M_w 4.4) the fit seems good while for the upper bound (M_w 7.4) the fit leaves much to be desired. For comparison, Figure 3 shows the corresponding plot for the distance metric ATSCA (compare Table 3) which was used by Atkinson and Silva (2000) for stochastic modeling of California ground motions. It is already visually apparent that the latter distance metric allows for a much better fit of the stochastic model. A fit visually similar to the one obtained for the distance metric of Atkinson and Silva (2000) was achieved by using the hypocentral distances (Fig. 4) that were calculated via the conversion relations of Scherbaum *et al.* (2004b).

At second glance, however, it is not too surprising that the distance metric used for the generation of an empirical ground-motion model does not perform as well when plugged into a stochastic model. The physical assumptions about how ground motion decays as a function of distance and magnitude are often very different, which will affect the choice of the optimum distance metric. In Figure 2 one can see, for example, that the use of rupture distance as distance metric for the stochastic model leads to a strong overprediction of the spectral values for large magnitudes and close Joyner-Boore (reference) distances. A distance metric that gives larger values for close Joyner-Boore distances will reduce this effect and result in a better overall fit. Consequently, we have tested the performance of seven different distance metrics in the context of stochastic modeling. The definitions of the individual metrics are given in Table 3. All distance conversions were performed by using the conversion relations of Scherbaum *et al.* (2004b). For RRMS and RRMSSEIS (Table 3), the distance metrics based on the rms distance of Kanamori (1993), which was proposed for use in strong motion modeling by Boatwright *et al.* (2003), the corresponding conversion relations were additionally developed according to the same procedure as described in Scherbaum *et al.* (2004b). Table 4 shows the resulting model parameters and the corresponding misfit values (bottom row) for all different distance metrics. Overall, the lowest misfit value was obtained based on the distance metric used by Atkinson and Silva (2000), followed by R_{hyp} and R_{rms}. From

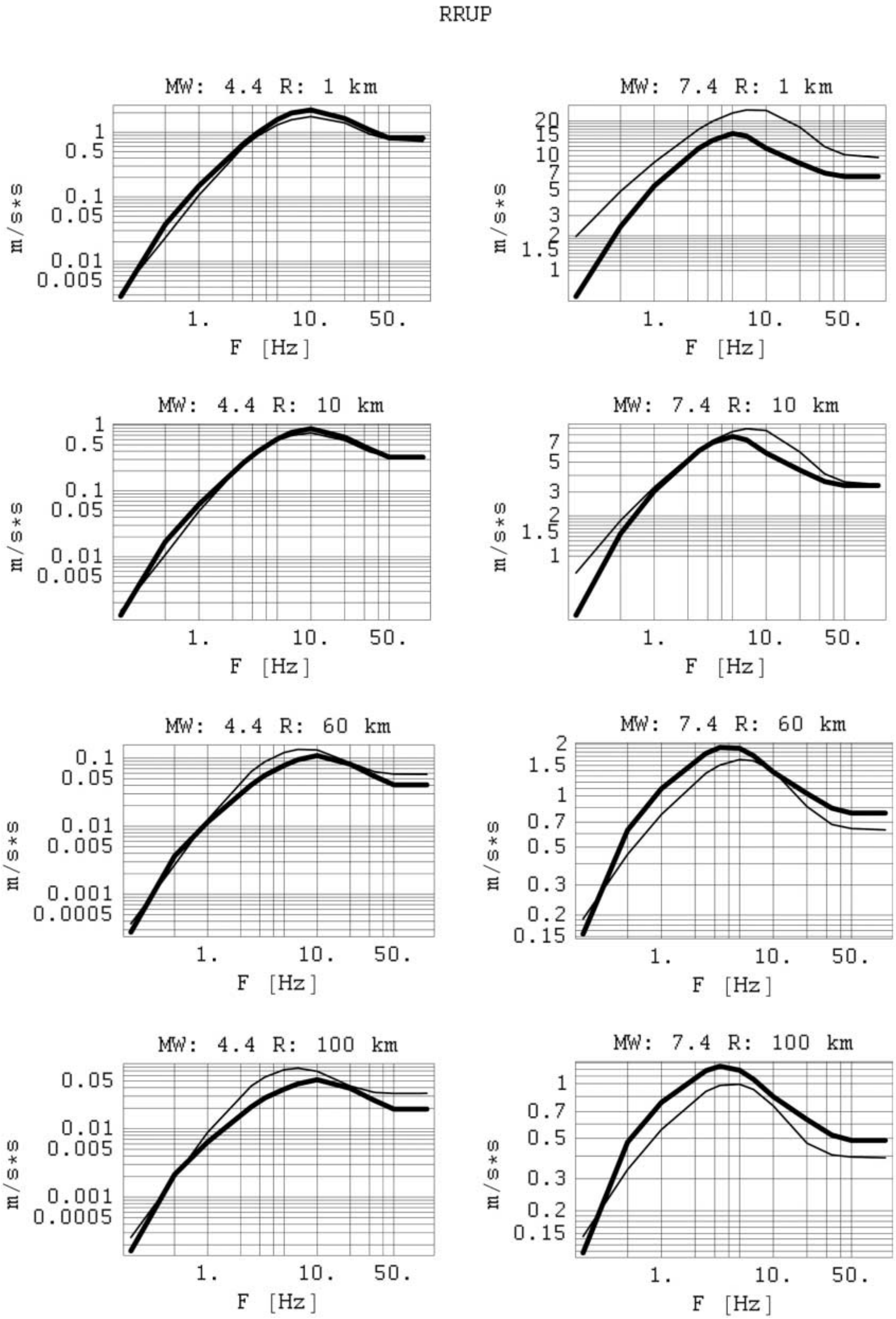

Figure 2. Model spectra for the optimum stochastic model (thin lines) and spectra calculated from the ground-motion prediction equation of Abrahamson and Silva (1997) (heavy lines) for selected magnitudes and Joyner-Boore distances (reference distance). For the stochastic model, the rupture distance was used as distance metric. The distance conversions from the Joyner-Boore reference distance to rupture distance was performed using the conversion relations of Scherbaum *et al.* (2004b).

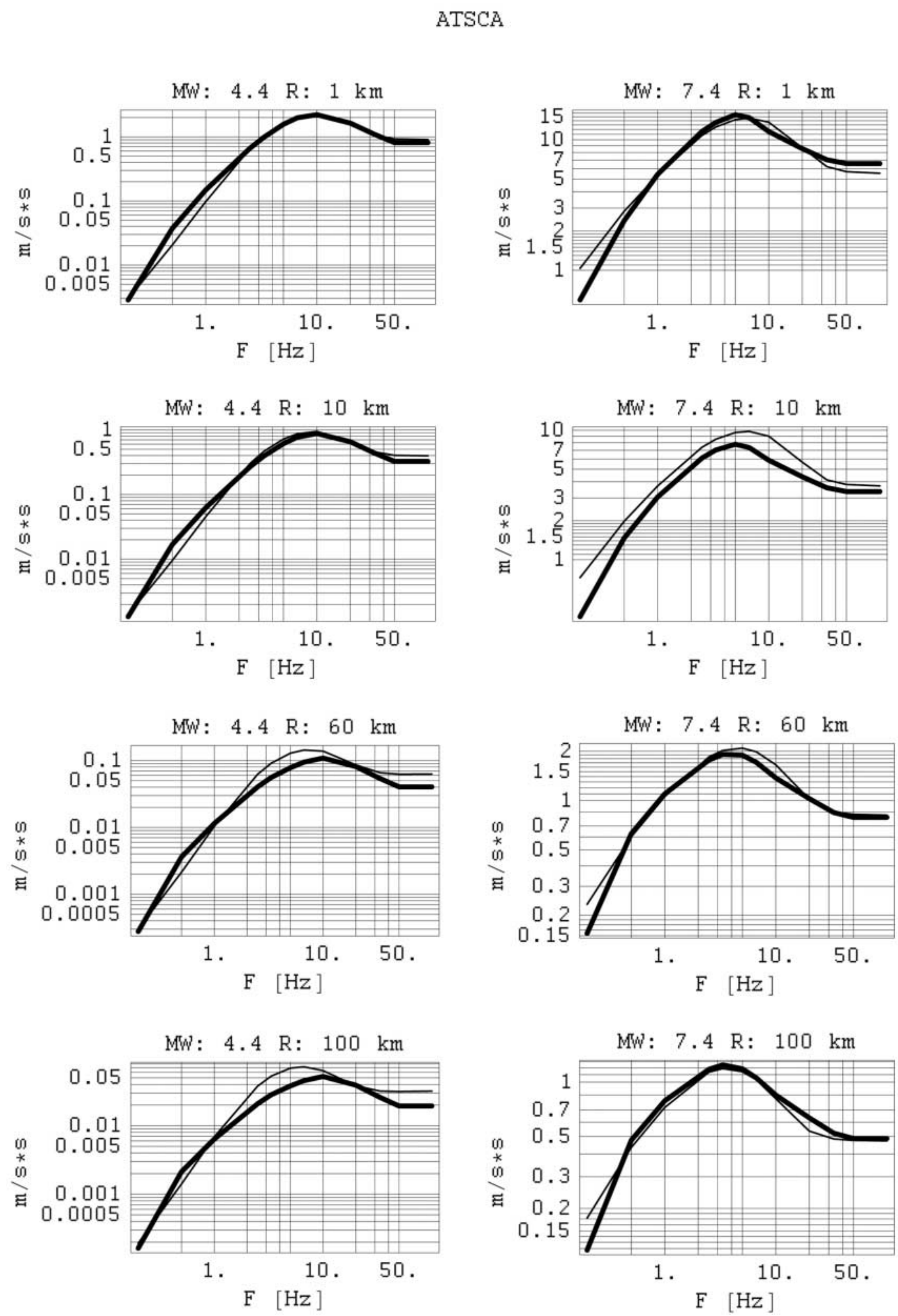

Figure 3. Model spectra for the optimum stochastic model (thin lines) and spectra calculated from the ground-motion prediction equation of Abrahamson and Silva (1997) (heavy lines) for selected magnitudes and Joyner-Boore distances (reference distance). For the stochastic model, the metric ATSCA (compare Table 3) was used.

Table 3
Different Distance Metrics Used for Stochastic Ground-Motion Modeling in the Present Study

Label	Metric	Comment
RHYP	R_{hyp}	Hypocentral distance
RRUP	R_{rup}	Distance to the closest point on the rupture plane
RSEIS	R_{seis}	Distance to the closest point on the seismogenic part of the rupture plane
ATSCA	$\sqrt{R_{\mathrm{rup}}^2 + h(M)^2}$	R_{rup} is the distance to the closest point on the rupture plane, $h(fM)$ is a magnitude-dependent pseudodepth (Atkinson and Silva, 2000).
ABRCA	$\sqrt{R_{\mathrm{JB}}^2 + 8^2}$	R_{JB} is the Joyner-Boore distance, the horizontal distance to the closest surface projection of the rupture plane. This distance metric has been used for Californian data (Abrahamson, personal comm., 2003).
RRMS	R_{rms}	Root-mean-square distance defined as $R_{\mathrm{rms}} = \frac{1}{\sqrt{\frac{1}{S}\int \frac{1}{R^2} \cdot dS}}$, where the integral is taken over the entire fault surface S (Kanamori *et al.*, 1993).
RRMSSEIS	R_{RMSSEIS}	Defined as $R_{\mathrm{rms}} = \frac{1}{\sqrt{\frac{1}{S_{\mathrm{seis}}}\int \frac{1}{R^2} \cdot dS}}$, where the integral is taken over the seismogenic part of the fault surface S_{seis}.

Table 4
Minimum Misfit Model Parameters Obtained for the Abrahamson and Silva (1997) Models for Different Distance Metrics

Parameter	Search Range	ABRCA	ATSCA	RHYP	RRMS	RRMSSEIS	RRUP	RSEIS	WNA
$\Delta\sigma$ (bar)	0.1 to 500	54	79	163	216	267	30	32	100
κ_0 (sec)	0 to 0.1	0.033	0.039	0.047	0.050	0.044	0.032	0.031	0.04
Q_0	50 to 1000	325	196	269	235	270	445	442	180
α	0 to 1.0	0.37	0.46	0.38	0.41	0.31	0.26	0.27	0.45
R_1 (km)	10 to 50	23.5	44.5	42.5	45.9	48.3	34.4	27.6	40
a_1	−0.8 to −1.2	−1.0	−1.0	−1.1	−1.0	−1.1	−0.87	−0.87	−1.0
R_2 (km)	max. 110	83.1	73.8	65.3	78.2	71.7	57.7	72.0	∞
a_2	−1 to 0.3	−0.75	−0.25	−0.78	−0.94	−0.58	−0.88	−0.91	−0.5
R_3 (km)	∞ (fixed)								
a_3	−0.5 (fixed)								
r	0.02 to 0.08	0.038	0.037	0.037	0.057	0.056	0.051	0.021	0.05
vs_{30} (m/sec)	450 to 1000	650	500	500	650	620	700	700	620
Misfit value		0.096	0.074	0.084	0.086	0.094	0.120	0.113	0.232

The bottom row gives the corresponding minimum residual values for the data set used for the inversion. The rightmost column corresponds to the WNA model of Campbell (2003) in conjunction with rupture distance.

Table 4 and Figures 3 and 4 it is apparent that a similar quality of fit can be reached with rather different model parameters. As a consequence, the latter cannot be interpreted separately from the distance metric with which the model was generated. Another reason for the necessity to interpret the stochastic parameters only as a whole set are the known tradeoffs between individual model parameters, for example, between stress drop, kappa, and attenuation (Scherbaum, 1990; Boore *et al.*, 1992). Table 4 also shows that in terms of overall fit (independent of the particular distance metric used) optimized stochastic host region models provide a much better representation for the Abrahamson and Silva (1997) model than the one obtained by using the WNA model of Campbell (2003) (last column in Table 4). This would probably be true for any other Western U.S. model as well, simply because the generating data set of the Abrahamson and Silva (1997) model is not purely Californian and our approach models data sets, not necessarily geographical regions.

Results

For all ground-motion models under study, optimum stochastic models were calculated for all distance metrics described in Table 3. Table 5 shows the corresponding minimum residual values for all combinations of ground-motion model and distance metric. The minimum misfit values obtained for each ground motion model are in boldface. Table 5 illustrates that the distance metrics yielding the best-fitting models differ from model to model. However, the hypocentral distance performs well for most investigated models, followed by the two types of rms-distance which

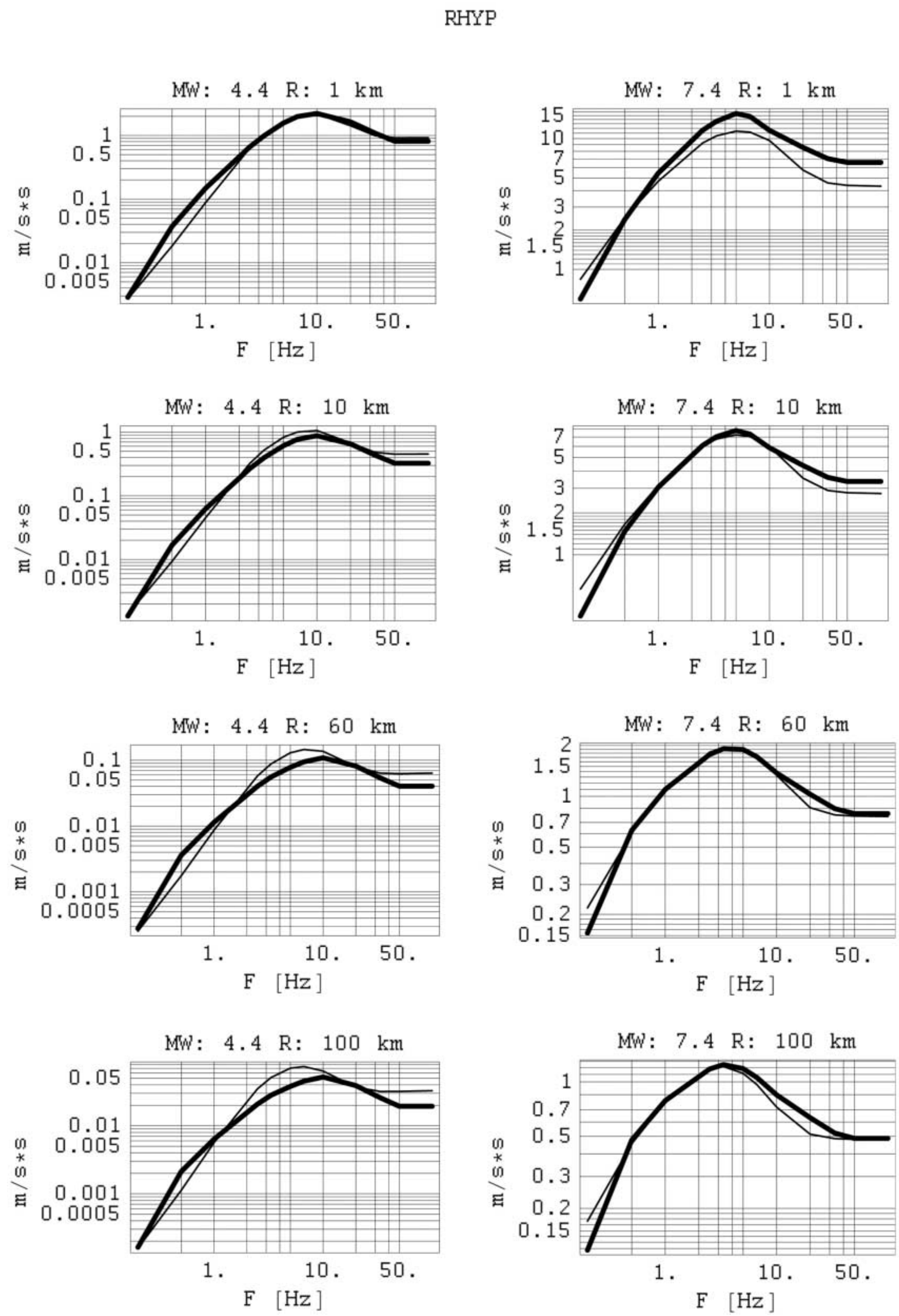

Figure 4. Model spectra for the optimum stochastic model (thin lines) and spectra calculated from the ground-motion prediction equation of Abrahamson and Silva (1997) (heavy lines) for selected magnitudes and Joyner-Boore distances (reference distance). The distance conversions from the reference distance to rupture distance, which is used by Abrahamson and Silva (1997), and the hypocentral distance (for the stochastic model) was performed using the conversion relations of Scherbaum *et al.* (2004b).

Table 5
Minimum Residual Values Obtained for Different Distance Metrics and Different Ground-Motion Prediction Equations

Model Name	ABRCA	ATSCA	RHYP	RRMS	RRMSSEIS	RRUP	RSEIS
Abrahamson and Silva (1997)	0.096	**0.074**	0.084	0.086	0.094	0.120	0.113
Ambraseys and Douglas (2003)	0.1689	0.0826	**0.0199**	0.0209	0.0201	0.2127	0.1894
Ambraseys *et al.* (1996)	0.080	0.088	0.103	0.108	0.104	0.057	**0.054**
Berge-Thierry *et al.* (2003)	0.0670	0.0491	**0.0452**	0.0529	0.0531	0.0950	0.0904
Boore *et al.* (1997)	0.0654	0.0678	**0.0303**	0.0398	0.0348	0.0727	0.0646
Campbell and Bozorgnia (2003a)	0.145	0.114	0.049	**0.038**	0.045	0.168	0.161
Lussou *et al.* (2001)	0.022	0.020	**0.019**	0.021	0.021	0.039	0.036
Sabetta and Pugliese (1996)	0.258	0.251	0.238	0.219	**0.203**	0.226	0.209
Spudich *et al.* (1999)	0.1434	0.1390	0.1286	**0.1256**	0.1257	0.1441	0.1433

The minimum misfit values for each ground-motion model are in boldface.

Table 6
Minimum Misfit Stochastic Model Parameters for the Ground-Motion Models under Study

Model Name	$\Delta\sigma$ (bar)	κ_0 (sec)	Q_0	α	R_1 (km)	a_1	R_2 (km)	a_2	r	vs_{30} (m/sec)
Abrahamson and Silva (1997)	163	0.047	269	0.38	42.5	−1.1	65.3	−0.78	0.037	500
Ambraseys and Douglas (2003)	132	0.038	52	0.785	44.6	−0.846	NA	NA	0.021	650
Ambraseys *et al.* (1996)	83	0.066	164	0.905	25.8	−0.8	85.8	−1.0	0.038	500
Berge-Thierry *et al.* (2003)	46	0.047	256	0.958	30.9	−0.979	68.9	−0.883	0.0377	450
Boore *et al.* (1997)	77	0.061	83	0.846	48.9	−0.8	82.2	−0.299	0.0623	450
Campbell and Bozorgnia (2003a)	63	0.042	130	0.534	24.4	−0.817	28.9	−0.505	0.0554	500
Lussou *et al.* (2001)	44	0.032	167	0.77	13.5	−1.02	73.3	−0.86	0.0266	550
Sabetta and Pugliese (1996)	68	0.042	87	0.856	42.3	−0.837	47.13	−0.836	0.0677	500
Spudich *et al.* (1999)	12	0.287	84	1.0	43.3	−0.807	63.1	−0.97	0.0442	450

The hypocentral distance was used as distance metric for the stochastic model. The geometrical spreading exponent a_3 up to infinity was set to 0.5, $\langle R_{\Theta\Phi}\rangle = 0.55$, $V = 1/\sqrt{2}$, $F = 2$. The density and velocity were set to $\rho_S = 2700$ kg/m^3 and $\beta_S = 3500$ m/sec.

were used. The good performance of the rms-distance was not totally unexpected because this distance measure was specifically defined to model spatial energy decay from extended sources (Kanamori *et al.*, 1993). The good performance of the hypocentral distance measure was more of a surprise at first. However, it could be explained by the results of two recent studies of hypocenter locations in finite-source models (Mai *et al.*, 2005; Manighetti *et al.*, 2005). Manighetti *et al.* (2005) suggest that there is a critical distance from a major asperity beyond which an earthquake does not nucleate. The maximum distance at which an earthquake can nucleate from the major asperity it eventually breaks is ~50% of its total length and width. Most earthquakes, however, seem to nucleate closer, with an hypocenter-asperity distance (HA) on the order of 20–30% of their total length or width. This average value is similar to the mean normalized size of major asperities within earthquake fault planes as determined from smaller data sets by Somerville *et al.* (1999) and Beresnev and Atkinson (2002). This suggests that earthquakes may actually nucleate at the edges of the major asperities that they eventually break. These results are in agreement with those of Mai *et al.* (2005) which indicate that hypocenters are often located either within or close to regions of large slip. Table 6 shows the minimum residual model parameters for the hypocentral distance as distance metric for the stochastic models. These sets of models are believed to represent the generating data sets of the investigated empirical ground-motion models rather than specific geographical regions.

Model Bias, Parameter Variability, and Parameter Correlation

The accuracy of ground-motion prediction using the hybrid empirical method is determined to a large degree by the quality of the best-fitting equivalent stochastic model. Even the best-fitting stochastic host-region models will show systematic differences between the ground-motion predictions from the empirical prediction equation and the corresponding equivalent stochastic model. These systematic differences are magnitude and frequency dependent and differ considerably between different ground-motion models (Figs. 5, 6, 7). In some cases we were able to find very well-fitting stochastic models for the whole range of magnitudes, distances, and frequencies for which the models are supposed to be valid (Abrahamson and Silva, 1997; Lussou *et al.*, 2001; Berge-Thierry *et al.*, 2003). For some ground-motion prediction relations, however, (e.g., Spudich *et al.*,

(*Text continues on page 442.*)

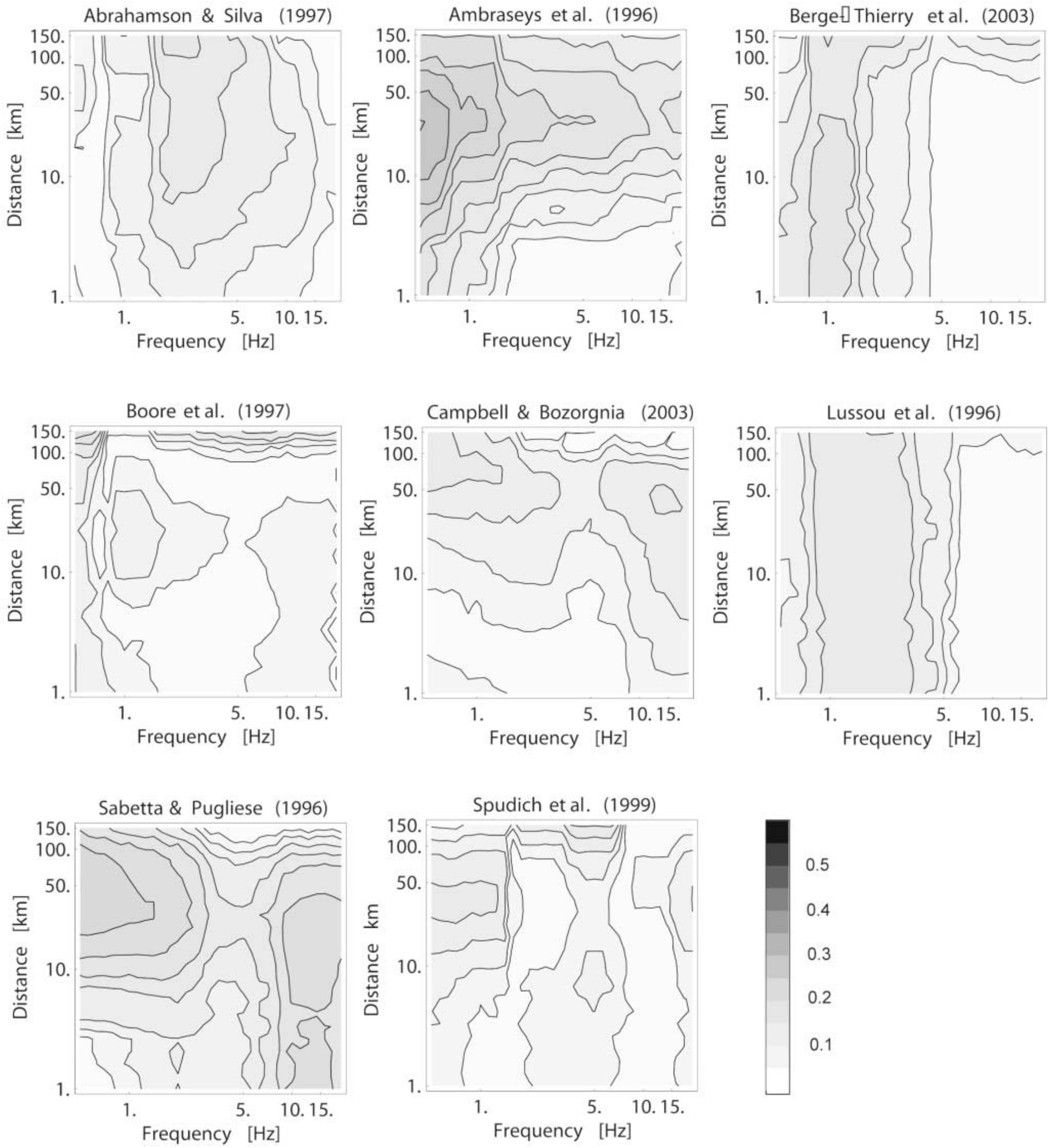

Figure 5. Systematic differences of the optimum stochastic models (for RHYP as distance metric) for an M_w 5.5 earthquake as function of frequency and Joyner-Boore distance. Displayed are the absolute values of differences between the $\log_{10}$ values of the response spectra generated from the optimum stochastic models and the $\log_{10}$ values of the spectra calculated from the different ground-motion prediction equations. The contour line spacing is 0.05. The distance conversions from the reference distance to the distance measures used by the empirical ground-motion models and to the hypocentral distance (for the stochastic model) was performed using the conversion relations of Scherbaum *et al.* (2004b).

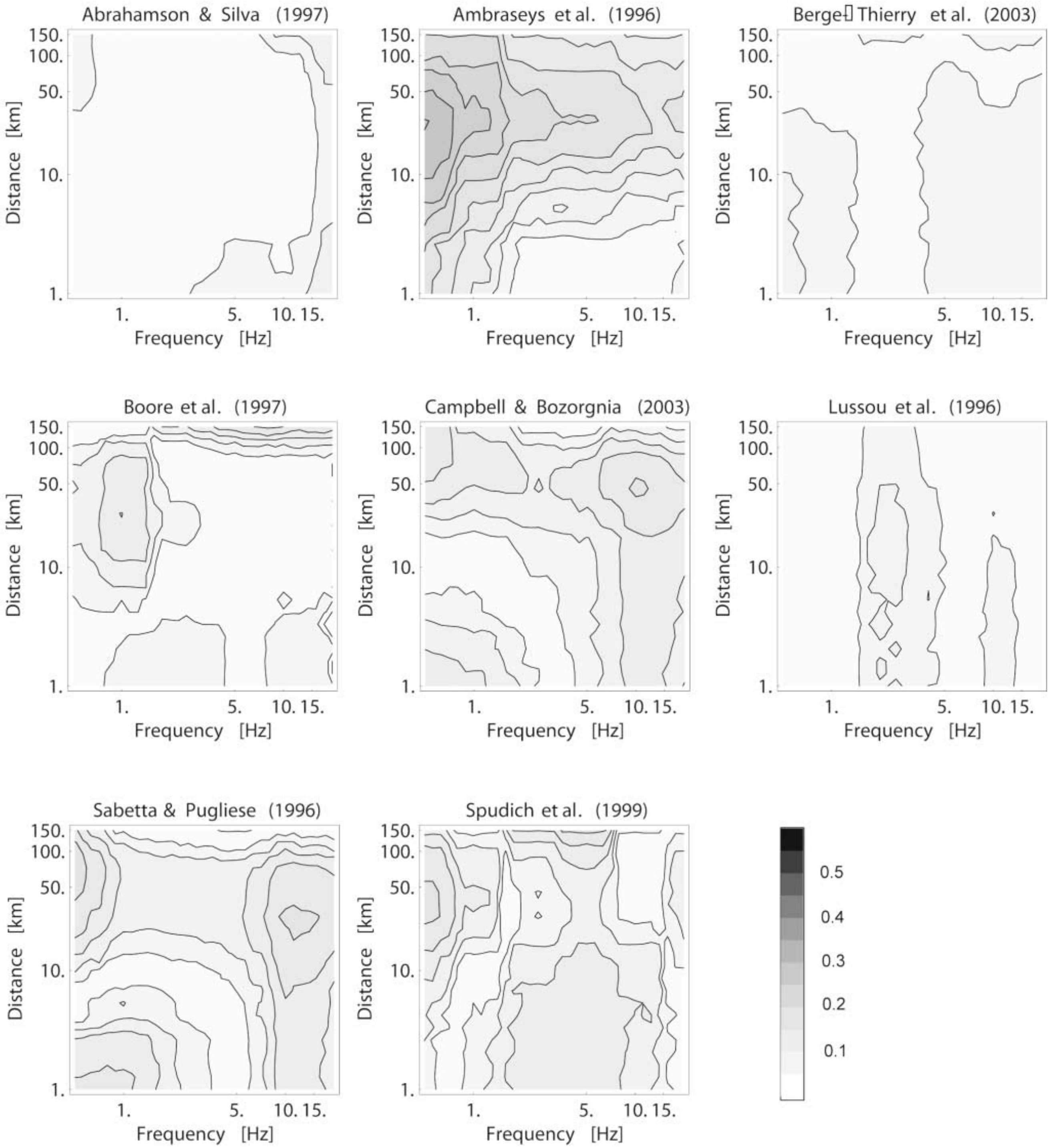

Figure 6. Systematic differences of the optimum stochastic models (for RHYP as distance metric) for an M_w 6.5 earthquake as function of frequency and Joyner-Boore distance. Displayed are the absolute values of differences between the $\log_{10}$ values of the response spectra generated from the optimum stochastic models and the $\log_{10}$ values of the spectra calculated from the different ground-motion prediction equations. The contour line spacing is 0.05. The distance conversions from the reference distance to the distance measures used by the empirical ground-motion models and to the hypocentral distance (for the stochastic model) was performed using the conversion relations of Scherbaum *et al.* (2004b).

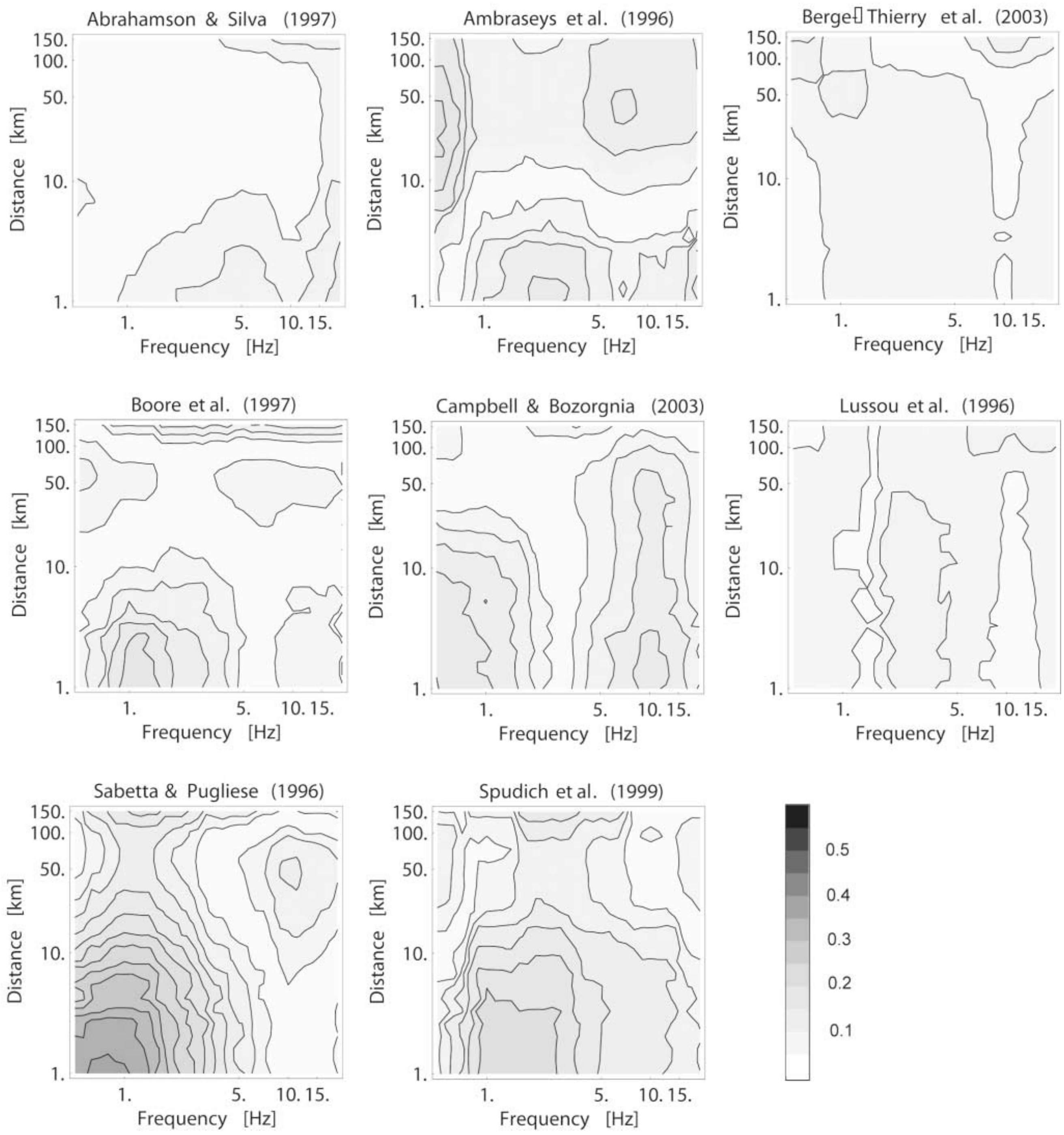

Figure 7. Systematic differences of the optimum stochastic models (for RHYP as distance metric) for an M_w 7.5 earthquake as function of frequency and Joyner-Boore distance. Displayed are the absolute values of differences between the $\log_{10}$ values of the response spectra generated from the optimum stochastic models and the $\log_{10}$ values of the spectra calculated from the different ground-motion prediction equations. The contour line spacing is 0.05. The distance conversions from the reference distance to the distance measures used by the empirical ground-motion models and to the hypocentral distance (for the stochastic model) was performed using the conversion relations of Scherbaum *et al*. (2004b).

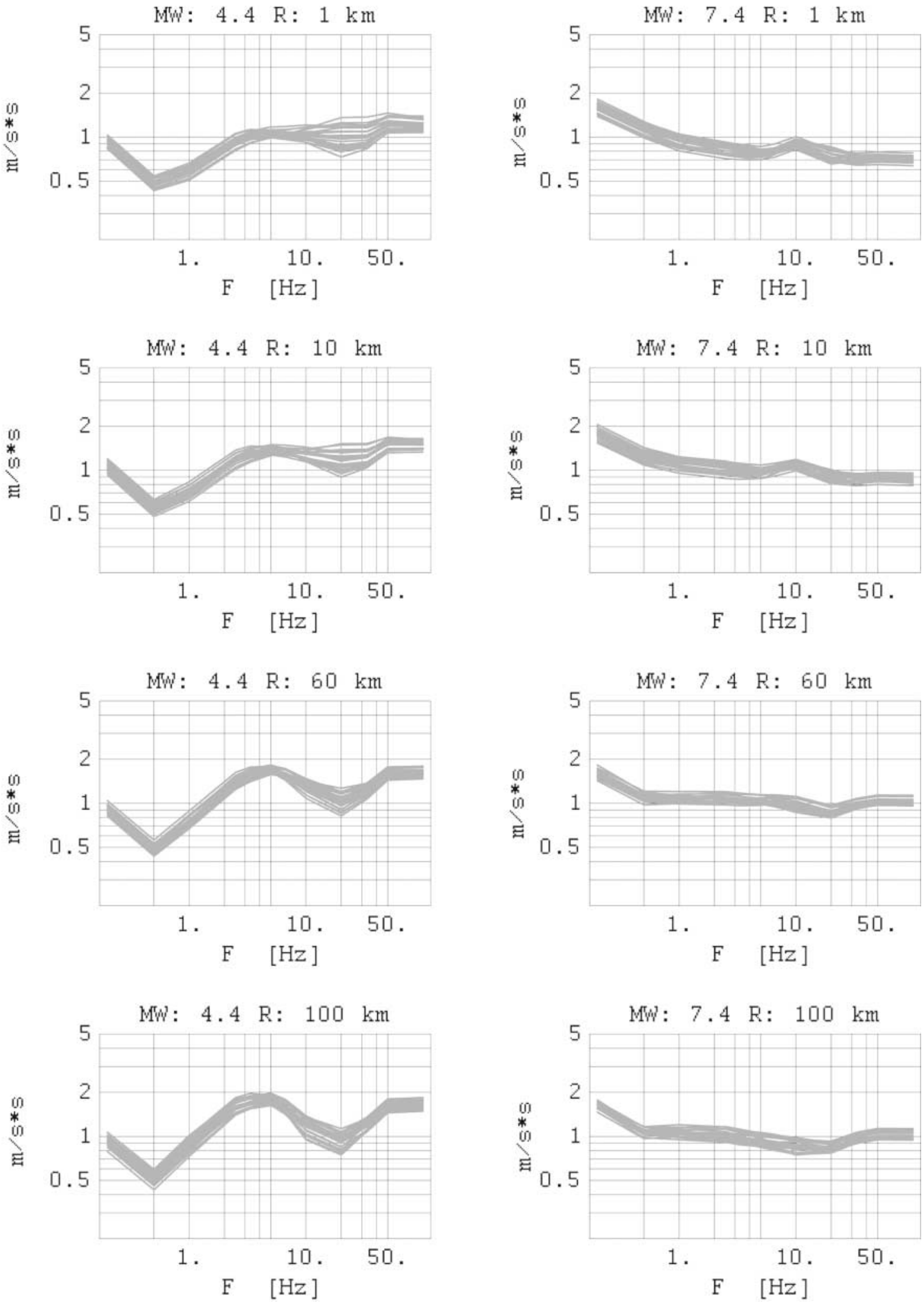

Figure 8. The thin gray lines show the 25 best-fitting stochastic model misfit spectra with respect to the Abrahamson and Silva prediction equation (1997), obtained from the genetic algorithm search for selected magnitudes and Joyner-Boore distances. The distance conversions from the reference distance to rupture distance, which is used by Abrahamson and Silva (1997), and the hypocentral distance (for the stochastic model) was performed using the conversion relations of Scherbaum *et al*. (2004b).

1999) even the best-fitting stochastic model spectra can show a rather large systematic deviation for certain magnitudes and/or distances. For the model of Spudich *et al.* (1999) this could be caused by the fact that the corresponding generating data set was selected based on stress regimes rather than geographic regions. For the majority of models under study, however, we would subjectively judge the fit as fair. These differences will map as additional variance onto the corresponding hybrid empirical ground-motion predictions (Scherbaum *et al.*, 2005).

In addition to the systematic bias, additional uncertainies in the final hybrid empirical model predictions will be produced by the variability of model parameters corresponding to those models that provide a similar fit. As an illustration of this effect, Figure 8 shows the 25 best-fitting stochastic model misfit spectra with respect to the Abrahamson and Silva prediction equation (1997), obtained from the genetic algorithm search, for selected magnitudes and Joyner-Boore distances. Based on the visual judgment of the size of the misfit as well as on the fact that the misfit between the best model and the 25th best model increases by only 7%, the whole set of models would be acceptable models. The corresponding model parameters show a noticeable spread as is displayed in Table 7. In the final predictions of a corresponding hybrid empirical model spectrum, this spread will cause additional uncertainty. However, because of trade-offs in the model parameters, it is important that these correlations are taken into account. Otherwise, the uncertainties in the model predictions of the hybrid model might be considerably overestimated as illustrated in Figure 9. One way of achieving this is the calculation of host-to-target conversion filters in which the host-region models are drawn by weighted Monte-Carlo sampling from a larger set of acceptable models with the weights being a function of the model misifit (Scherbaum *et al.*, 2005). A comprehensive discussion of source of uncertainties in a hybrid empirical model for central Europe is given by Scherbaum *et al.* (2005).

Table 7
Model Parameter Spread for the 25 Best-Fitting Models for the Abrahamson and Silva (1997) Ground-Motion Prediction Equation (Compare Fig. 8)

Parameter	Best Model	Mean for 25 Best Models	Standard Deviation for 25 Best Models
$\Delta\sigma$ (bar)	163	188	27.7
κ_0 (sec)	0.047	0.042	0.007
Q_0	269	286	115.5
α	0.38	0.34	0.17
R_1 (km)	42.5	38.2	10.3
a_1	−1.1	−1.04	0.03
R_2 (km)	65.3	66.7	16.2
a_2	−0.78	−0.73	0.26
r	0.037	0.053	0.015
vs_{30} (m/sec)	500	673	127

The hypocentral distance is used as distance metric. The misfit increase between the best model and the 25th best model is approximately 7%.

Conclusion

Campbell's hybrid empirical approach (Campbell, 2003, 2004) provides a methodological framework to adapt ground-motion prediction equations to arbitrary target regions. As a key element in the necessary host-to-target-region conversions, we have calculated equivalent stochastic host-region models for several popular empirical ground-motion prediction equations for shallow crustal earthquakes. Because a variety of different distance measures have been proposed for this purpose, we have compared their performance in terms of overall quality of fit. As a result, for each empirical ground-motion model we obtain a whole set of stochastic models together with their misfit values. For most of the empirical ground-motion models, we obtain equivalent stochastic models that match the empirical models within the full magnitude and distance ranges of their generating data sets fairly well. However, the overall quality of fit and the resulting model parameter sets strongly depend on the particular choice of the distance metric used for the stochastic model. Although there is no single distance metric providing the lowest misfit stochastic models for all empirical equations, the hypocentral distance performs best in most cases. This is compatible with the results of a recent study of hypocenter locations in finite-source models which indicates that hypocenters are often located either within or close to regions of large slip (Mai *et al.*, 2005; Manighetti *et al.*, 2005). It must be emphasized that minimum-misfit stochastic models match data sets but not necessarily geographical regions. This is because, for good reasons, essentially all empirical ground-motion prediction equations contain data from different geographical regions. Even the best-fitting stochastic models will result in a magnitude- and frequency-dependent systematic bias which, according to the laws of uncertainty propagation, will increase the variance of the corresponding hybrid empirical model predictions (Scherbaum *et al.*, 2005). As a consequence, the selection of empirical ground-motion models for host-to-target-region conversions requires considerable judgment of the ground-motion analyst. The model parameters of the set of "good fitting stochastic models" are highly correlated, which should be accounted for as well if the corresponding effects on hybrid empirical model predictions using any of these equations are to be evaluated. For this purpose, the set of model parameters and misfit values for the 100 best-fitting stochastic models for each ground-motion model under study (Table 2), as well as the conversion coefficients for the rms-distances (RRMS and RRMSSEIS) are available on request from the first author (fs@geo.uni-potsdam.de).

Acknowledgments

This article is contribution EG2/DT-04 from a series of studies inspired by participation in the Pegasos project (Abrahamson *et al.*, 2002). We thank the following people for providing a stimulating environment and continuous support for the development of the ideas presented herein: Philip Birkhäuser, Jim Farrington, Andreas Hölker, Philippe Roth, and

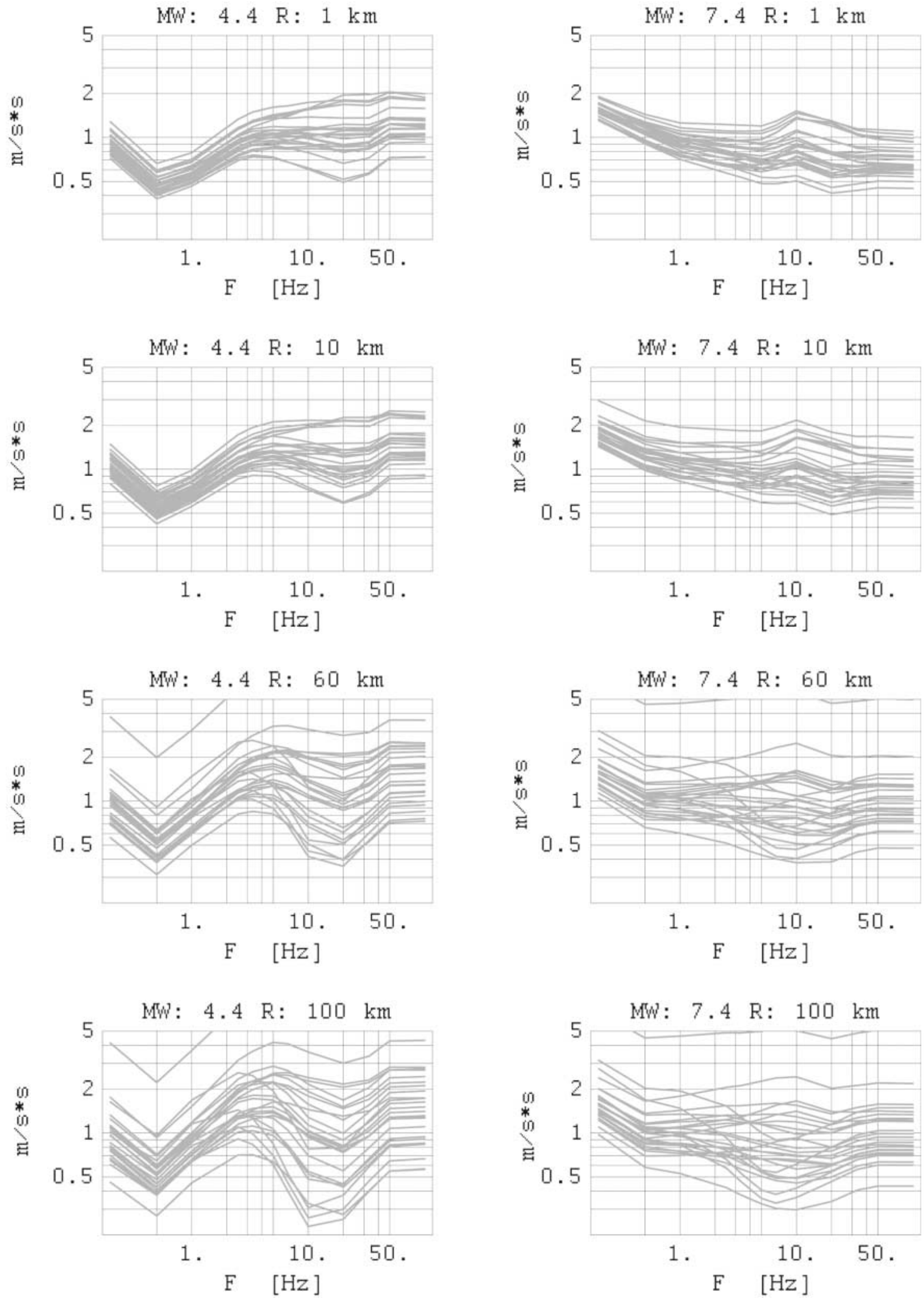

Figure 9. The effect of wrongly assuming that the individual model parameters are independent. The thin gray lines show 25 stochastic model misfit spectra with respect to the Abrahamson and Silva prediction equation (1997), obtained by randomly drawing the individual model parameters from the set of the 25 best-fitting models shown in Figure 8. The distance conversions from the reference distance to rupture distance, which is used by Abrahamson and Silva (1997), and the hypocentral distance (for the stochastic model) was performed using the conversion relations of Scherbaum *et al.* (2004b).

Christian Sprecher. Frank Scherbaum and Fabrice Cotton are especially thankful for the numerous discussions with Julian Bommer, Hilmar Bungum, Fabio Sabetta, and Norm Abrahamson. We also thank John Douglas, Dave Boore, Stefano Parolai, Ken Campbell, and Gail Atkinson for their comments on the manuscript and Anthony Lomax for generously providing us with his code.

References

Abrahamson, N. A., and K. M. Shedlock (1997). Overview, *Seism. Res. Lett.* **68,** no. 1, 9–23.

Abrahamson, N. A., and W. J. Silva (1997). Empirical response spectral attenuation relations for shallow crustal earthquakes, *Seism. Res. Lett.*, **68,** no. 1, 94–127.

Abrahamson, N. A., P. Birkhauser, M. Koller, D. Mayer-Rosa, P. M. Smit, C. Sprecher, S. Tinic, and R. Graf (2002). PEGASOS—A comprehensive probabilistic seismic hazard assessment for nuclear power plants in Switzerland, Paper presented at the 12 European Conference on Earthquake Engineering, London.

Ambraseys, N. N., and J. Douglas (2003). Near-field horizontal and vertical ground motions, *Soil Dyn. Earthquake Eng.* **23,** 1–18.

Ambraseys, N. N., K. A. Simpson, and J. J. Bommer (1996). Prediction of horizontal response spectra in Europe, *Earthquake Eng. Struct. Dyn.* **25,** 371–400.

Anderson, J. G., and S. E. Hough (1984). A model for the shape of the Fourier amplitude spectrum of acceleration at high frequencies, *Bull. Seism. Soc. Am.* **74,** 1969–1993.

Atkinson, G. M., and W. Silva (1997). An empirical study of earthquake source spectra for California earthquakes, *Bull. Seism. Soc. Am.* **87,** 97–113.

Atkinson, G. M., and W. Silva (2000). Stochastic modeling of California ground motions, *Bull. Seism. Soc. Am.* **90,** no. 2, 255–274.

Bay, F., D. Fäh, L. Malagnini, and D. Giardini (2003). Spectral shear-wave ground-motion scaling in Switzerland, *Bull. Seism. Soc. Am.* **93,** no. 1, 414–429.

Beresnev, I. A., and G. M. Atkinson (2002). Source parameters of earthquakes in eastern and western North America, *Bull. Seism. Soc. Am.* **92,** no. 2, 695–710.

Berge-Thierry, C., F. Cotton, O. Scotti, D. A. Griot-Pommera, and Y. Fukushima (2003). New empirical response spectral attenuation laws for moderate European earthquakes, *J. Earthquake Eng.* **7,** no. 2, 193–222.

Boatwright, J., H. Bundock, J. Luetgert, L. C. Seekins, L. Gee, and P. Lombard (2003). The dependence of PGA and PGV on distance and magnitude inferred from Northern California ShakeMap data, *Bull. Seism. Soc. Am.* **93,** 2043–2055.

Bommer, J. J., N. A. Abrahamson, F. O. Strasser, A. Pecker, P. Y. Bard, H. Bungum, F. Cotton, D. Fäh, F. Sabetta, F. Scherbaum, and J. Studer (2004). The challenge of defining upper bounds on earthquake ground motions, *Seism. Res. Lett.* **75,** no. 1, 82–95.

Bommer, J. J., F. Scherbaum, H. Bungum, F. Cotton, F. Sabetta, and N. A. Abrahamson (2005). On the use of logic trees for ground-motion prediction equations in seismic hazard analysis, *Bull. Seism. Soc. Am.* **95,** no. 2, 377–389.

Boore, D. (2000). SMSIM-Fortran programs for simulating ground motions from earthquakes, Version 2.0, A revision of OFR 96-80-A (No. A revision of USGS OFR00-509), http://geopubs.wr.usgs.gov/open-file/of00-509/ (last accessed January 2006).

Boore, D. M. (1983). Stochastic simulation of high-frequency ground motions based on seismological models of the radiated spectra, *Bull. Seism. Soc. Am.* **73,** no. 6, 1865–1894.

Boore, D. M. (1986). Short-period P- and S-wave radiation from large earthquakes: implications for spectral scaling relations, *Bull. Seism. Soc. Am.* **76,** no. 1, 43–64.

Boore, D. M. (2003). Simulation of ground motion using the stochastic method, *Pageoph* **160,** 635–676.

Boore, D. M., and G. M. Atkinson (1987). Stochastic prediction of ground motion and spectral response parameters at hard-rock sites in eastern North America, *Bull. Seism. Soc. Am.* **77,** no. 2, 440–467.

Boore, D. M., and W. B. Joyner (1984). A note on the use of random vibration theory to predict peak amplitudes of transient signals, *Bull. Seism. Soc. Am.* **74,** no. 5, 2035–2039.

Boore, D. M., and W. B. Joyner (1997). Site amplifications for generic rock sites, *Bull. Seism. Soc. Am.* **87,** no. 2, 327–341.

Boore, D. M., W. B. Joyner, and T. E. Fumal (1997). Equations for estimating horizontal response spectra and peak acceleration from western North American earthquakes: a summary of recent work, *Seism. Res. Lett.* **68,** no. 1, 128–153.

Boore, D. M., W. B. Joyner, and L. G. Wennerberg (1992). Fitting the stochastic omega^{-2} source model to observed response spectra in western North America: trade-offs between Delta sigma and kappa, *Bull. Seism. Soc. Am.* **82,** no. 4, 1956–1963.

Brune, J. N. (1970). Tectonic stress and the spectra of seismic shear waves from earthquakes, *J. Geophys. Res.* **76,** no. 26, 4997–5009.

Brune, J. N. (1971). Tectonic stress and the spectra of seismic shear waves from earthquakes, Correction, *J. Geophys. Res.* **76,** no. 20, 5002.

Campbell, K. W. (2003). Prediction of strong ground motion using the hybrid empirical method and its use in the development of ground-motion (attenuation) relations in Eastern North America, *Bull. Seism. Soc. Am.* **93,** no. 3, 1012–1033.

Campbell, K. W. (2004). Erratum to Prediction of strong ground motion using the hybrid empirical method and its use in the development of ground-motion (attenuation) relations in Eastern North America, *Bull. Seism. Soc. Am.* **94,** no. 6, 2418.

Campbell, K. W., and Y. Bozorgnia (2003a). Updated near-source ground-motion attenuation relations for the horizontal and vertical components of peak ground acceleration and acceleration response spectra, *Bull. Seism. Soc. Am.* **93,** no. 1, 314–331.

Campbell, K. W., and Y. Bozorgnia (2003b). Erratum to Updated near-source ground-motion attenuation relations for the horizontal and vertical components of peak ground acceleration and acceleration response spectra, *Bull. Seism. Soc. Am.* **93,** no. 3, 1413.

Campbell, K. W., and Y. Bozorgnia (2003c). Erratum to Updated near-source ground-motion attenuation relations for the horizontal and vertical components of peak ground acceleration and acceleration response spectra, *Bull. Seism. Soc. Am.* **93,** no. 4, 1872.

Campbell, K. W., and Y. Bozorgnia (2004). Erratum to Updated near-source ground-motion attenuation relations for the horizontal and vertical components of peak ground acceleration and acceleration response spectra, *Bull. Seism. Soc. Am.* **94,** no. 6, 2417.

Chen, S.-Z., and G. M. Atkinson (2002). Global comparisons of earthquake source spectra, *Bull. Seism. Soc. Am.* **92,** no. 3, 885–895.

Cotton, F., F. Scherbaum, J. J. Bommer, and H. Bungum (2006). Criteria for selecting and adjusting ground-motion models for specific target regions: application to Central Europe and rock sites, *J. Seism.* (in press).

Douglas, J. (2003). Earthquake ground motion estimation using strong-motion records: a review of equations for the estimation of peak ground acceleration and spectral ordinates, *Earth Sci. Rev.* **61,** 43–104.

Gentile, F., F. Pettenati, and L. Sirovich (2004). Validation of the automatic nonlinear source inversion of the U.S. Geological Survey intensities of the Whittier Narrows 1987 earthquake, *Bull. Seism. Soc. Am.* **94,** 1737–1747.

Goldberg, D. E. (1989). *Genetic Algorithms in Search, Optimization, and Machine Learning*, Addison-Wesley, Reading, Massachusetts.

Hanks, T. C. (1979). b-values and $\omega^{-\gamma}$ seismic source models: implications for tectonic stress variations along active crustal fault zones and the estimations of high-frequency strong ground motions, *J. Geophys. Res.* **84,** no. B5, 2235–2242.

Hanks, T. C., and R. K. McGuire (1981). The character of high-frequency strong ground motion, *Bull. Seism. Soc. Am.* **71,** no. 6, 2071–2095.

Hernandez, B., F. Cotton, and M. Campillo (1999). Contribution of radar interferometry to a two-step inversion of the kinematic process of the 1992 Landers earthquake, *J. Geophys. Res.* **104,** 13,083–13,099.

Kanamori, H., J. Mori, E. Hauksson, T. Heaton, L. K. Hutton, and L. M. Jones (1993). Determination of earthquake energy release and Ml using Terrascope, *Bull. Seism. Soc. Am.* **83,** no. 2, 330–346.

Kramer, S. L. (1996). *Geotechnical Earthquake Engineering*, Prentice-Hall, Upper Saddle River, New Jersey.

Kulkarni, R. B., R. R. Youngs, and K. J. Coppersmith (1984). Assessment of confidence intervals for results of seismic hazard analysis, Paper presented at the 8th World Conference on Earthquake Engineering, San Francisco.

Lomax, A., and R. Snieder (1994). Finding sets of acceptable solutions with a genetic algorithm with application to surface wave group dispersion in Europe, *Geophys. Res. Lett.* **21,** no. 24, 2617–2620.

Lomax, A., and R. Snieder (1995). Identifying sets of accetable solutions to non-linear geophysical inverse problems which have complicated misfit functions, *Nonlinear Proc. Geophys.* **2,** 222–227.

Lussou, P., P. Y. Bard, F. Cotton, and Y. S. Fukushima (2001). Seismic design regulation codes: contribution of K-Net data to site effect evaluation, *J. Earthquake Eng.* **5,** no. 1, 13–33.

Mai, P. M., P. Spudich, and J. Boatwright (2005). Hypocenter locations in finite-source rupture models, *Bull. Seism. Soc. Am.* **95,** no. 3, 965–980.

Malagnini, L., R. B. Herrmann, B. M. Di, and K. Koch (1999). Ground motion attenuation at regional distance in Italy and Germany, *Seism. Res. Lett.* **70,** no. 2, 214.

Malagnini, L., R. B. Herrmann, and K. Koch (2000). Regional ground-motion scaling in central Europe, *Bull. Seism. Soc. Am.* **90,** no. 4, 1052–1061.

Manighetti, I., M. Campillo, C. Sammis, P. M. Mai, and G. King (2005). Evidence for self-similar, triangular slip distributions on earthquakes: implications for earthquake and fault mechanics, *J. Geophys. Res.* **110,** doi 10.1029/2004JB003174.

Margaris, B. N., and D. M. Boore (1998). Determination of $\Delta\sigma$ and κ_0 from response spectra of large earthquakes in Greece, *Bull. Seism. Soc. Am.* **88,** no. 1, 170–182.

McGuire, R. K., and T. C. Hanks (1980). RMS accelerations and spectral amplitudes of strong ground motion during the San Fernando, California earthquake, *Bull. Seism. Soc. Am.* **70,** no. 5, 1907–1919.

Ou, G.-B., and R. B. Herrmann (1990). A statistical model for ground motion produced by earthquakes at local and regional distances, *Bull. Seism. Soc. Am.* **80,** no. 6, 1397–1417.

Raoof, M., R. B. Herrmann, and L. Malagnini (1999). Attenuation and excitation of three-component ground motion in Southern California, *Bull. Seism. Soc. Am.* **89,** no. 4, 888–902.

Reiter, L. (1990). *Earthquake Hazard Analysis: Issues and Insights*, Columbia University Press, New York.

Sabetta, F., and A. Pugliese (1996). Estimation of response spectra and simulation of nonstationary earthquake ground motion, *Bull. Seism. Soc. Am.* **86,** no. 2, 337–352.

Scherbaum, F. (1990). Combined inversion for the three-dimensional Q structure and source parameters using microearthquake spectra, *J. Geophys. Res.* **95,** no. B8, 12,423–12,438.

Scherbaum, F., J. J. Bommer, H. Bungum, F. Cotton, and N. A. Abrahamson (2005). Composite ground-motion models and logic trees: methodology, sensitivities, and uncertainties, *Bull. Seism. Soc. Am.* **95,** no. 5, 1575–1593.

Scherbaum, F., F. Cotton, and P. Smit (2004a). On the use of response spectral-reference data for the selection of ground-motion models for seismic hazard analysis: the case of rock motion, *Bull. Seism. Soc. Am.* **94,** no. 6, 2164–2185.

Scherbaum, F., J. Schmedes, and F. Cotton (2004b). On the conversion of source-to-site distance measures for extended earthquake source models, *Bull. Seism. Soc. Am.* **94,** no. 3, 1053–1069.

Somerville, P., K. Irikura, R. Graves, S. Sawada, D. Wald, N. Abrahamson, Y. Iwasaki, T. Kagawa, N. Smith, and A. Kowada (1999). Characterizing crustal earthquake slip models for the prediction of strong ground motion, *Seism. Res. Lett.* **70,** no. 1, 59–80.

Spudich, P., W. B. Joyner, A. G. Lindh, D. M. Boore, B. M. Margaris, and J. B. Fletcher (1999). SEA99: A revised ground motion prediction relation for use in extensional tectonic regimes, *Bull. Seism. Soc. Am.* **89,** no. 5, 1156–1170.

Stoffa, P. L., and M. K. Sen (1991). Nonlinear multiparameter optimization using genetic algorithms: Inversion of plane wave seismograms, *Geophysics* **56,** no. 11, 1794–1810.

Institut für Geowissenschaften
Universität Potsdam
P.O. Box 601553
D-14415, Potsdam, Germany
fs@geo.uni-potsdam.de
(F.S., H.S.)

Laboratoire de Géophysique Interne et Tectonophysique
Université Joseph Fourier
BP 53
F-38041, Grenoble, France
fabrice.cotton@obs.ujf-grenoble.fr
(F.C.)

Manuscript received 28 January 2005.